14.1   A MULTI-SEASON STUDY OF THE EFFECTS OF MODIS SEA-SURFACE TEMPERATURES ON OPERATIONAL WRF FORECASTS AT NWS MIAMI, FL

Jonathan L. Case*[1], Pablo Santos[2], Michael E. Splitt[3], Steven M. Lazarus[3], Kevin K. Fuell[4], Stephanie L. Haines[4], Scott R. Dembek[5], and William M. Lapenta[6]

[1]ENSCO Inc./Short-term Prediction Research and Transition (SPoRT) Center, Huntsville, AL
[2]NOAA/NWS Miami, Miami, FL
[3]Florida Institute of Technology, Melbourne, FL
[4]University of Alabama – Huntsville/SPoRT Center, Huntsville, AL
Universities Space Research Association/SPoRT Center, Huntsville, AL
[6]NASA/SPoRT Center, Huntsville, AL

1. INTRODUCTION

Studies at the NASA Short-term Prediction Research and Transition (SPoRT) Center have suggested that the use of Moderate Resolution Imaging Spectroradiometer (MODIS) sea-surface temperature (SST) composites in regional weather forecast models can have a significant positive impact on short-term numerical weather prediction in coastal regions. Recent work by LaCasse *et al.* (2007) highlights lower atmospheric differences in regional numerical simulations over the Florida offshore waters using 2-km SST composites derived from the MODIS instrument aboard the polar-orbiting Aqua and Terra Earth Observing System satellites. To help quantify the value of this impact on NWS Weather Forecast Offices (WFOs), the SPoRT Center and the NWS WFO at Miami, FL (MFL) are collaborating on a project to investigate the impact of using the high-resolution MODIS SST fields within the Weather Research and Forecasting (WRF) prediction system.

The project's goal is to determine whether more accurate specification of the lower-boundary forcing within WRF will result in improved land/sea fluxes and hence, more accurate evolution of coastal mesoscale circulations and the associated sensible weather elements over a multi-seasonal time frame. The remainder of this paper is organized as follows. Section 2 described the operational WRF configuration as run at NWS MFL. Section 3 provides a description of the SST products used in Control and experimental WRF simulations. The experimental design is discussed in Section 4 while preliminary results are presented in Section 5. The paper concludes with future work, acknowledgements, and references in Sections 6–8, respectively.

2. OPERATIONAL WRF CONFIGURATION AT NWS MFL

The NWS MFL is currently running the WRF system in real-time to support daily forecast operations, using the National Centers for Environmental Prediction (NCEP) Nonhydrostatic Mesoscale Model (NMM, Janjić *et al.* 2001) dynamical core within the NWS Science and Training Resource Center's Environmental

Modeling System (EMS) software. The EMS is a stand-alone modeling system capable of downloading the necessary daily datasets, and initializing, running and displaying WRF forecasts in the NWS Advanced Weather Interactive Processing System (AWIPS) with little intervention required by forecasters. More information on the EMS software can be found in the online user's guide at http://strc.comet.ucar.edu/wrf/wrf_userguide.htm.

The model physics used within the NMM dynamical core in the NWS MFL runs consist of the modified Kain-Fritsch convective parameterization scheme (Kain 2004) for determining sub-grid scale convective processes and the Ferrier microphysics scheme as used operationally in the NCEP North American Mesoscale (NAM) model (Ferrier *et al.* 2002). The Geophysical Fluid Dynamics Laboratory schemes are used for computing shortwave (Lacis and Hansen 1974) and longwave radiation processes (Fels and Schrawzkopf 1975; Schwarzkopf and Fels 1985; Schwarzkopf and Fels 1991). Planetary boundary layer and turbulence processes are parameterized by the Mellor-Yamada-Janjić scheme (Janjić 1990, 1996, 2002). The Noah land surface model (LSM, Ek *et al.* 2003) is used to calculate energy exchanges between the land surface and the planetary boundary layer. Surface-layer calculations of friction velocities and exchange coefficients needed for the determination of sensible and latent fluxes in the Noah LSM are provided by the NCEP Eta similarity theory scheme (Janjić 1996, 2002).

Twenty-seven hour forecasts are run daily with start times of 0300, 0900, 1500, and 2100 UTC on a domain with 4-km horizontal grid spacing covering the southern half of Florida and the far western portions of the Bahamas, the Florida Keys, the Straights of Florida, and adjacent waters of the Gulf of Mexico and Atlantic Ocean (Figure 1). Each model run is initialized using the Local Analysis and Prediction System (LAPS) analyses available in AWIPS, invoking the diabatic "hot-start" capability. In this WRF model "hot-start", the LAPS-analyzed cloud and precipitation features are converted into model microphysics fields with enhanced vertical velocity profiles, effectively reducing the model spin-up time required to predict precipitation systems. The SSTs are initialized with the NCEP Real-Time Global (RTG) analyses at 1/12° resolution (~9 km); however, the RTG product does not exhibit fine-scale details consistent with its grid resolution.

Corresponding author address: Jonathan Case, ENSCO, Inc., 320 Sparkman Dr., Room 3062, Huntsville, AL, 35805. Email: Jonathan.Case-1@nasa.gov

3. SST COMPOSITE PRODUCTS

3.1 Real-time global (RTG) SST (Control)

Currently, the highest-resolution, continuous global SST products available consist of the 1/12° Real-Time Global (RTG) product generated by the National Centers for Environmental Prediction (NCEP) (Thiébaux et al. 2003, defined above) and the 1/20° Operational Sea Surface Temperature and Sea Ice Analysis (OSTIA) product developed by the National Centre for Ocean Forecasting (Stark et al. 2007). The operational EMS software has the capability to download and interpolate the 1/12° RTG product to initialize the WRF sea surface; therefore, this dataset is the one used in the Control configuration of our experiment.

3.2 MODIS SST Composite (Experimental)

A 1-km MODIS SST composite, produced at the NASA SPoRT Center, was created by combining multiple passes of the EOS MODIS SST data (Haines et al. 2007). The compositing assumes that the day-to-day variation of SST is relatively small — the degree to which this assumption is valid will likely vary spatially and seasonally. Data from both the Terra and Aqua platforms were combined to create separate day/night composites. The composites were created using the five most recent clear-sky SST values for each pixel. Daytime (nighttime) passes through the composite region occur at approximately 1600 and 1900 UTC (0400 and 0700 UTC), respectively. The compositing method used the warmest three of the five pixels in order to mitigate the impact of cloud contamination. Prior to being interpolated to the WRF simulation grid, each 1-km MODIS SST composite was sub-sampled to a coarser grid with 2-km horizontal grid spacing.

4. EXPERIMENT DESIGN

SPoRT conducted parallel WRF EMS runs identical to the operational configuration at NWS MFL except for the use of MODIS SST composites in place of the RTG product as the initial and boundary conditions over water. During an early phase of the experiment, problems in the initial temperature and wind fields from LAPS were found. These problems had been subjectively noticed by NWS MFL forecasters, but not documented in any objective manner until now. Upon confirmation of this problem, the LAPS analyses at WFO Miami no longer impose any balancing constraint prior to model initialization. Forecasters report that the change over this winter season has resulted in a noticeable improvement in model initialization. However, for the purposes of this experiment and given our inability to rerun the LAPS analyses for the study period, the LAPS analyses were excluded for this experiment entirely. Instead, the initial WRF fields were derived entirely from the 3-h NCEP NAM forecasts for both the Control and MODIS SST runs.

The incorporation of the MODIS SST composites into the SPoRT WRF runs was staggered such that the 0400 UTC composite initialized the 0900 UTC WRF, the 0700 UTC composite initialized the 1500 UTC WRF, the 1600 UTC composite initialized the 2100 UTC WRF, and the 1900 UTC composite initialized the 0300 UTC WRF. From mid-February to August 2007, 733 parallel WRF simulations were collected for analysis and verification: 189 at 0300 UTC, 184 at 0900 UTC, 182 at 1500 UTC, and 178 at 2100 UTC.

Surface verification statistics will be calculated at 57 land stations and 19 marine stations as shown in Figure 1. Statistics included root mean square error (RMSE) and bias for the 2-m temperature, 2-m dewpoint, 10-m wind speed, 10-m u- and v-wind components, and sea surface temperature. The statistics are to be computed separately for the land and marine stations since the marine stations might show more impact than the land stations. The SST has already been verified at the 6 buoy and C-MAN stations depicted by the filled boxes in Figure 1.

In addition to the verification statistics, the coauthors have begun to examine several individual cases in which the MODIS SST fields might have the most impact on the WRF predictions. The initial focus has been on easterly flow regimes where rain showers have developed offshore and impacted the Miami county warning region. The potential impacts of the MODIS SSTs on predictions of temperatures, moisture, convergent boundaries, and precipitation patterns are being documented.

5. PRELIMINARY RESULTS

5.1 Sample SST and Latent Heat Flux Difference Fields

Figure 2 and Figure 3 show plots of WRF-initialized RTG SSTs, MODIS SSTs, and latent heat flux differences from a sample forecast during Spring (1500 UTC 21 March) and late summer (1500 UTC 18 August), respectively. What becomes immediately apparent is the difference in the level of detail of the initial SST fields in both examples. In the SST initialization from 21 March, the RTG SST shows a smoothly-varying field with ~4°C temperature increase from north to south off the west coast of Florida and only ~1°C variation off the east coast and little variation around the shallower waters of the western Bahamas (Figure 2a). In contrast to the RTG plot, the MODIS-initialized SSTs show a very distinctive gradient of 2–3°C over a short distance on either side of the well-defined Gulf Stream current from the Florida Straits south of the Keys to the east of the Florida east coast (Figure 2b). A narrow wedge of cool SSTs is found hugging the east coast to the north of Lake Okeechobee over the Florida-Hatteras Shelf, coinciding with the location of buoy B1114 in Figure 1. Noticeably cooler MODIS SSTs are also found in the shallows of the western Bahamas. Overall, the largest differences in SST are well-correlated within the regions of the shallowest ocean bottom topography (not shown).

These differences in SSTs translate directly into variations in the latent heat fluxes over the water grid points. The difference in the 12-hour simulated latent heat flux (Figure 2c) shows as much as 100 W m^{-2} or more reduction in the latent heat flux over the cooler shelf waters near the Florida peninsula and western Bahamas, along with a simultaneous increase in latent

heat flux of comparable magnitude over the well-defined Gulf Stream region. Such variations in heat fluxes over small distances can lead to simulated mesoscale circulations that may not be resolved by predictions initialized with the much smoother RTG SST field. The authors are beginning to examine several different WRF simulations under easterly flow/showery weather regimes to diagnose the possible impacts of the MODIS SSTs throughout the period of record.

In the 18 August comparison given in Figure 3, the MODIS SST field (panel b) again shows more structure than the RTG field (panel a), although the differences are not quite as substantial as in the 21 March example. An examination of the difference field in 12-h simulated latent heat flux shows a very similar pattern as in the 21 March example, except with the opposite sign in most parts of the domain (Figure 3c). Over the shallower waters of the western Bahamas and off the southwest coast of Florida, the MODIS SSTs are now warmer than the RTG and the subsequent latent heat flux is larger. Meanwhile, the MODIS SSTs are slightly cooler over the Gulf Stream current, contrary to the 21 March example. The only exceptions to this sign change are found over Lake Okeechobee and the immediate shelf waters of the Florida east coast, north of Lake Okeechobee. In those locations, the MODIS SSTs and corresponding latent heat fluxes are still lower than the simulation using the RTG SSTs.

These results suggest that the MODIS SST composite is better able to capture the regional and (to an extent) seasonal variations in SST gradients, which are closely tied to the relative depths of the ocean around the Florida peninsula, Florida Keys, and western Bahamas. An examination of weekly or monthly mean SSTs throughout the period of record would help support this claim, and will be one of the next steps in our analysis.

5.2 SST Verification

The MODIS composites improve upon the RTG errors in nearly all months during the period of record (February to August 2007) for the 0300 and 2100 UTC WRF initialization times, which correspond to the 1900 UTC and 1600 UTC MODIS composite times, respectively. The initial SST RMSE is reduced the most substantially in February and July, but also improves in March, April, and August (Figure 4a and d). The spring months from April to June tend to have little or no reduction in the RMSE.

The largest improvements in initial SST RMSE is found at buoy B1114, located within the region of cool shelf waters to the east of the central Florida east coast (refer to location in Figure 1). In every month except for May, the RMSE is reduced by as much as 1°C or more in all model initialization times (Figure 4). The RMSE improvement is directly attributed to a reduction in the positive RTG bias at this station (Figure 5). In every model cycle, the RTG SST is too warm at buoy B1114 and the MODIS SST composite reduces this bias (sometimes too much as in the case of May and especially in the 1500 UTC forecast cycle).

There are a few instances when the MODIS SST RMSE increased over the RTG initialization. Both the 0900 and 1500 UTC forecast cycles had larger SST RMSE (Figure 4b and c) and negative biases (Figure 5b and c) from May to July, especially during the period from mid-June to mid-July (not shown). The possible causes of larger errors during these times and specific model initialization times could be as follows:

- Cloud contamination/latency problems in the MODIS SST compositing technique, particularly in the mid-June to mid-July time frame (Haines *et al.* 2007).
- The time difference between the MODIS composite and the model initialization. The 0700 UTC composite in particular may not be representative of the sea surface at the 1500 UTC model initialization time due to diurnal fluctuations in the SST.

The latency/cloud contamination problem during June and July can be inferred from the time series of SST initializations at Long Key, FL (LONF1, Figure 6). From mid-June through ~12 July, the MODIS SSTs are consistently too cold compared to observations and the RTG values, during a time of rapid increase in SSTs. During this time frame, there are several-day periods when the MODIS SST is nearly constant at LONF1, suggesting a latency problem possibly caused by extensive cloudiness. The MODIS SST composite "jumps" up to the observed values by 13 July, but still experiences nearly constant values for a time during the latter part of July. An examination of the 0400 UTC MODIS latency plot from 9 July indeed show that large latencies on the order of 2 weeks or more exists in the 9 July composite around the Florida Keys (Figure 7a). Therefore, much of the data in the MODIS SST composite was as old as 2 weeks or more. Meanwhile, in the 14 July composite, the latencies over the Florida Keys improves dramatically to only a few days or less (Figure 7b). The problems in the nighttime composites during the summer months could be related to the fact that most diurnal convection occurs over water during the nighttime hours, thereby reducing the overall quality of the nocturnal MODIS composites.

The mean MODIS, RTG, and observed SSTs, and the RMSE and biases for the entire period of record are summarized as a function of forecast cycle in Table 1. The mean MODIS SST (FBAR MODIS) best matches the mean observed values (OBAR) in the 0300 UTC and 2100 UTC forecasts. In both of these forecast cycles, the MODIS RMSE is slightly smaller than the RTG. The MODIS SSTs do tend to be negatively biased, however, in each forecast cycle except for the 0300 UTC cycle, probably partially due to the time lag between the MODIS composite and the model initialization time.

As described earlier, the largest SST cold bias at 1500 UTC could be caused by the 0700 UTC nighttime composite not being representative of the skin temperatures at 1500 UTC. The run-to-run variations that can result from the different MODIS composites are illustrated in Figure 8, which shows the MODIS–RTG simulated latent heat flux difference fields from the 1500 UTC and 2100 UTC WRF cycles on 14 June, both valid at 0900 UTC 15 June. Based on the verification results presented as well as these difference plots, it appears that the 0700 UTC SST composite used to initialize the

1500 UTC WRF was too cool in most of the model domain, as the latent heat flux difference is negative over most water locations in Figure 8a. Meanwhile in Figure 8b, the latent heat flux difference fields from the 2100 UTC WRF (using the 1600 UTC MODIS composite) depicts a more expected pattern of variations. The combination of latency and representativeness problems may have led to the poorest SST verification for the 1500 UTC WRF cycle using the 0700 UTC MODIS composite.

Given of the limitations in overpass times of the MODIS satellites and the time required to produce the composite, an alternative solution could be to initialize the 1500 UTC WRF SSTs with the 1600 UTC MODIS composite from the previous day. This could help improve the representativeness of the SSTs for this forecast cycle, given that the diurnal variation in SST may be more substantial than the day-to-day variations at a particular time. In addition, the quality of the MODIS composites could be improved during convectively active months by supplementing the MODIS data with passive microwave measurements, which would help improve SST observations over regions with extensive cloud contamination.

6. FUTURE WORK

Our future efforts in this project will consist of completing the surface verification of atmospheric variables over land and water stations, including accumulated precipitation. We will examine specific cases throughout the period of record in which possible forecast improvements can be discerned by using the high-resolution MODIS SST composites. Also, 1500 UTC WRF simulations could be made for some cases using 1600 UTC MODIS SST composites from the previous day in order to see how this improves the representation of SSTs at this model initialization time. Finally, SPoRT and NWS MFL seek to implement an operational solution of initializing WRF with the MODIS SST composites at the Miami WFO, based on the results of this study.

## 7. ACKNOWLEDGEMENTS/DISCLAIMER

8. REFERENCES

Ek, M. B., K. E. Mitchell, Y. Lin, E. Rogers, P. Grunmann, V. Koren, G. Gayno, and J. D. Tarpley, 2003: Implementation of Noah land surface model advances in the National Centers for E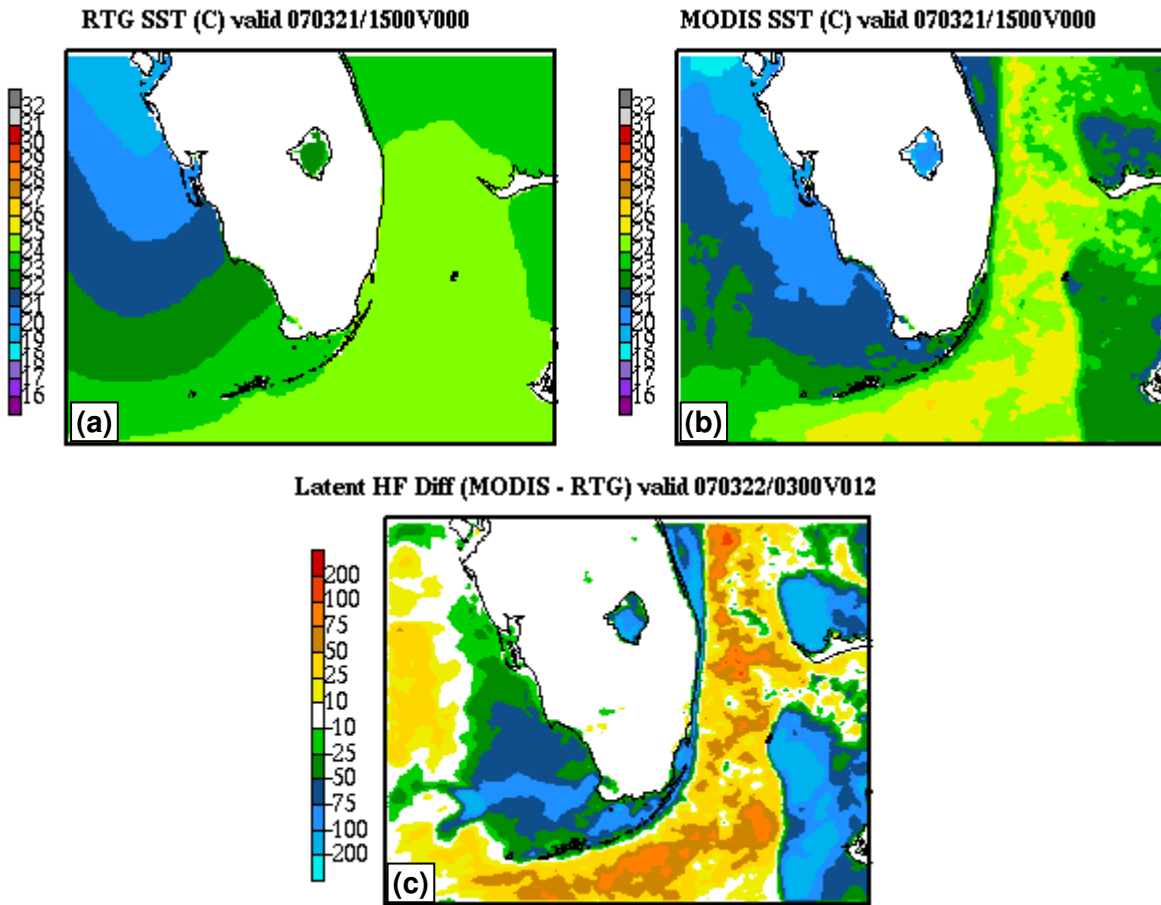nvironmental Prediction operational mesoscale Eta model. *J. Geophys. Res.,* **108 (D22),** 8851, doi:10.1029/2002JD003296.

Fels, S. B., and M. D. Schwarzkopf, 1975: The simplified exchange approximation: A new method for radiative transfer calculations. *J. Atmos. Sci.,* **32,** 1475-1488.

Ferrier, B. S., Y. Lin, T. Black, E. Rogers, and G. DiMego, 2002: Implementation of a new grid-scale cloud and precipitation scheme in the NCEP Eta model. Preprints, *15th Conf. on Numerical Weather Prediction,* San Antonio, TX, Amer. Meteor. Soc., 280-283.

Haines, S. L., G. J. Jedlovec, and S. M. Lazarus, 2007: A MODIS sea surface temperature composite for regional applications. *IEEE Trans. Geosci. Remote Sens.,* **45,** 2919-2927.

Janjić, Z. I., 1990: The step-mountain coordinate: Physical package. *Mon. Wea. Rev.,* **118,** 1429–1443.

Janjić, Z. I., 1996: The surface layer in the NCEP Eta Model. Preprints, *Eleventh Conference on Numerical Weather Prediction,* Norfolk, VA, Amer. Meteor. Soc., 354–355.

Janjić, Z. I., 2002: Nonsingular Implementation of the Mellor–Yamada Level 2.5 Scheme in the NCEP Meso model, NCEP Office Note, No. 437, 61 pp.

Janjić, Z. I., J. P. Gerrity, Jr., and S. Nickovic, 2001: An alternative approach to nonhydrostatic modeling. *Mon. Wea. Rev.,* **129,** 1164-1178.

Kain, J. S., 2004: The Kain-Fritsch convective parameterization: An update. *J. Appl. Meteor.,* **43,** 170-181.

LaCasse, K. M., M. E. Splitt, S. M. Lazarus, and W. M. Lapenta, 2007: The impact of high resolution sea surface temperatures on short-term model simulations of the nocturnal Florida marine boundary layer. *Mon Wea. Rev.,* In Press.

Lacis, A. A., and J. E. Hansen, 1974: A parameterization for the absorption of solar radiation in the earth's atmosphere. *J. Atmos. Sci.,* **31,** 118-133.

Schwarzkopf, M. D., and S. B. Fels, 1985: Improvements to the algorithm for computing CO2 transmissivities and cooling rates. *J. Geophys. Res.*, **90,** 541-550.

Schwarzkopf, M. D., and S. B. Fels, 1991: The simplified exchange method revisited: An accurate, rapid method for computations of infrared cooling rates and fluxes. *J. Geophys. Res.*, **96,** 9075-9096.

Stark, J. D., C. J. Donlon, M. J. Martin, and M. E. McCulloch, 2007: OSTIA: An Operational, high resolution, real time, global sea surface temperature analysis system. Preprints, *Oceans '07,* Aberdeen, Scotland, IEEE/OES, paper 061214-029. [Available online at http://ghrsst-pp.metoffice.com/pages/latest_analysis/docs/Stark_et_al_OSTIA_description_Oceans07.pdf]
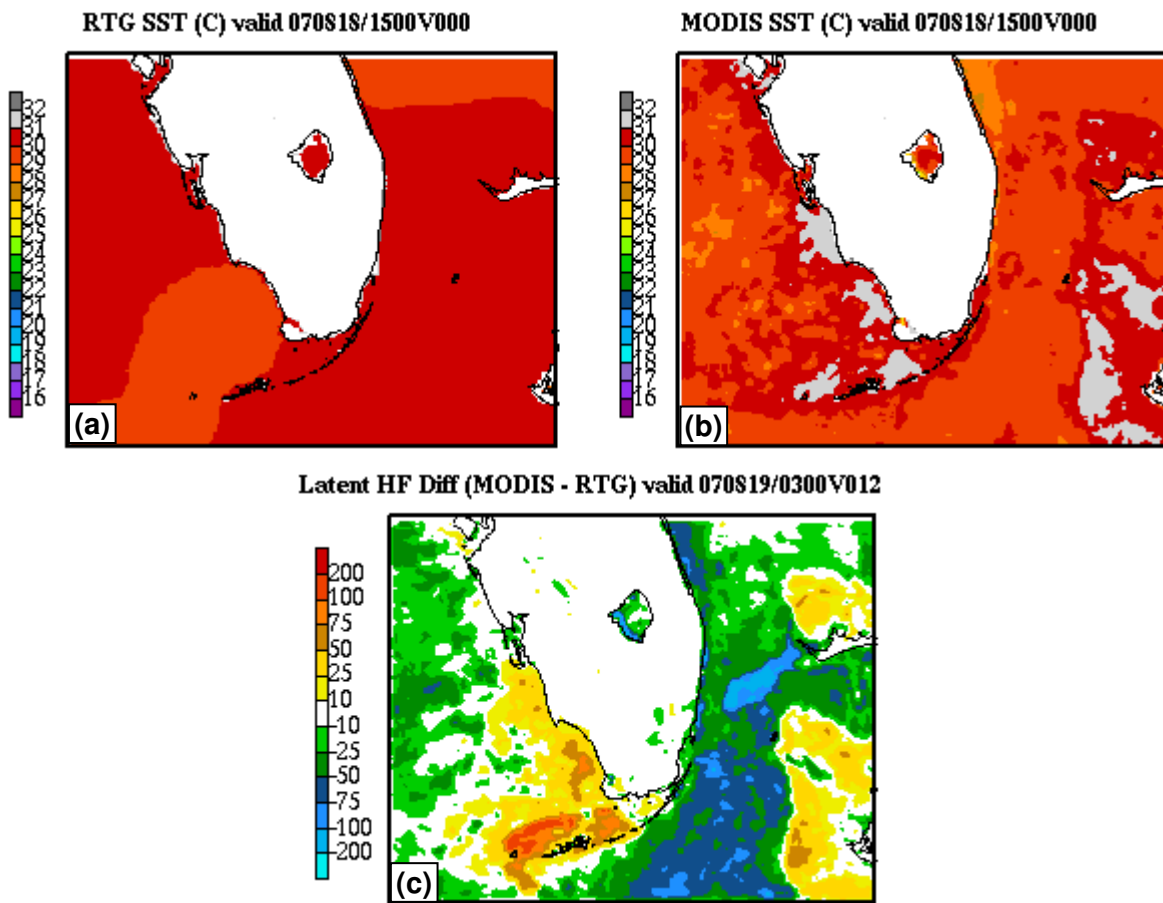
Thiébaux, J., E. Rogers, W. Wang, and B. Katz, 2003:
A new high-resolution blended global sea surface
temperature analysis. *Bull. Amer. Meteor. Soc.,* **84,**
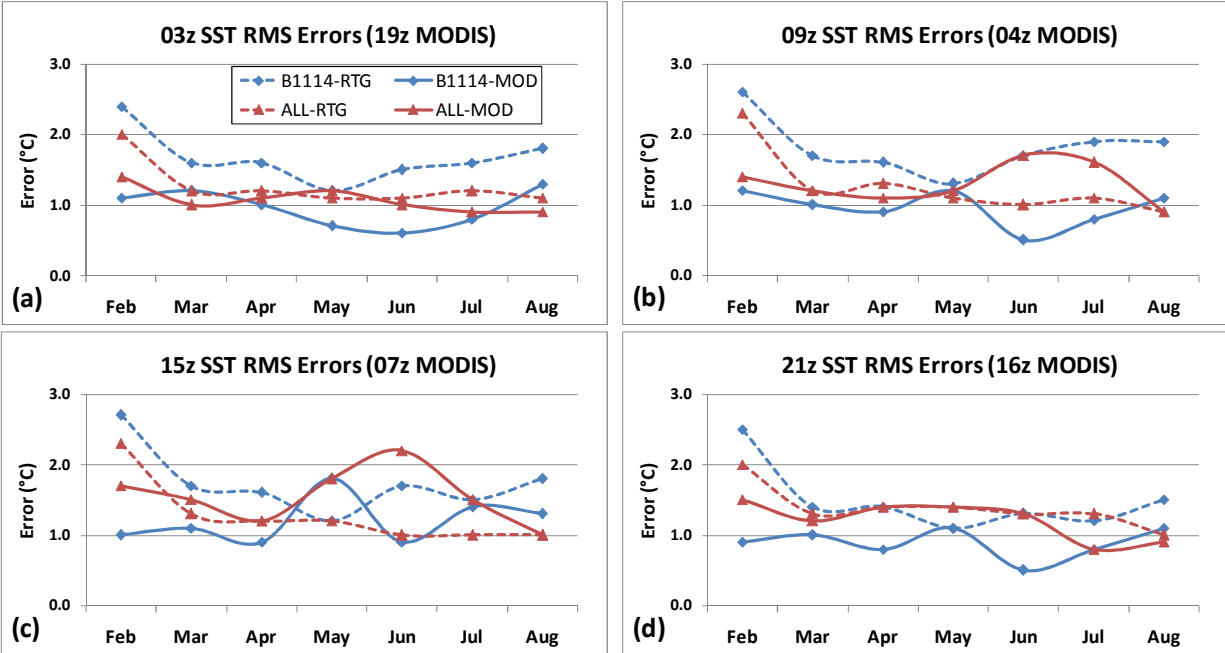645–656.

Surface Verification Sites
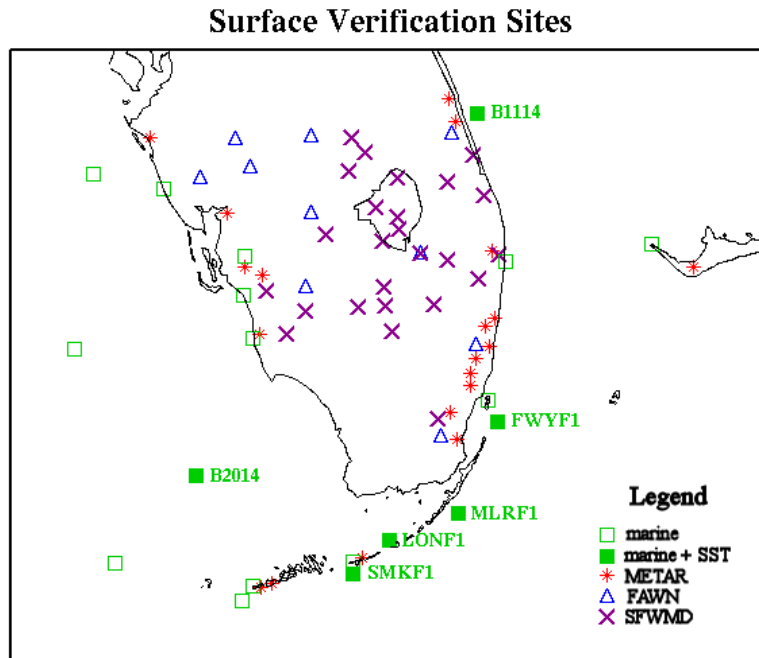
Figure 1. Surface stations used for verification of WRF model
forecasts, including land stations [METAR, Florida Automated Weather
Network (FAWN), and South Florida Water Management District
(SFWMD)], and marine sites [buoys and Coastal-Marine Automated
Network (C-MAN)].

RTG SST (C) valid 070321/1500V000

MODIS SST (C) valid 070321/1500V000

Latent HF Diff (MODIS - RTG) valid 070322/0300V012

Figure 2. SSTs in the WRF simulation initialized at 1500 UTC 21 March 2007 for (a) the 1/12° RTG SST product, and (b) the MODIS composite. (c) Difference in 12-hour forecast latent heat flux (W m^{-2}) between the MODIS and RTG WRF simulations, valid at 0300 UTC 22 March 2007.

RTG SST (C) valid 070818/1500V000

MODIS SST (C) valid 070818/1500V000

Latent HF Diff (MODIS - RTG) valid 070819/0300V012

Figure 3.   Same as in Figure 2, except showing the forecast initialized at 1500 UTC 18 August 2007.

Figure 4. Monthly sea surface temperature root mean square errors for all 6 marine stations labeled in Figure 1, and buoy B1114 on the Florida east coast at model initialization times (a) 0300 UTC, (b) 0900 UTC, (c) 1500 UTC, and (d) 2100 UTC.
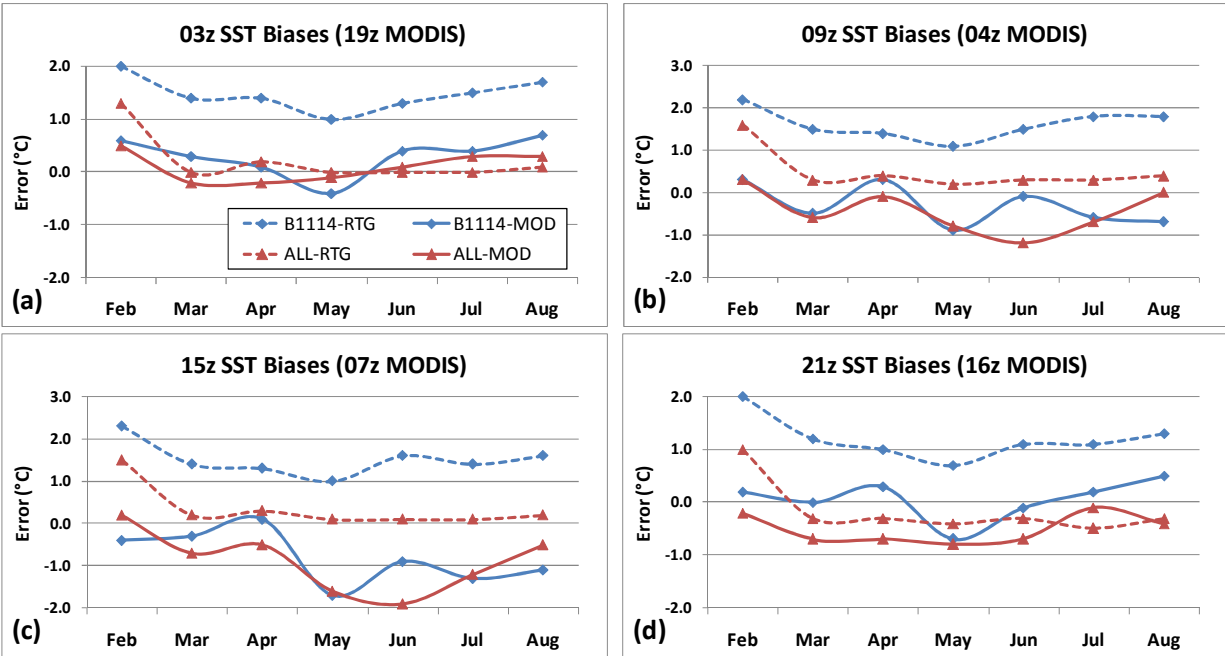
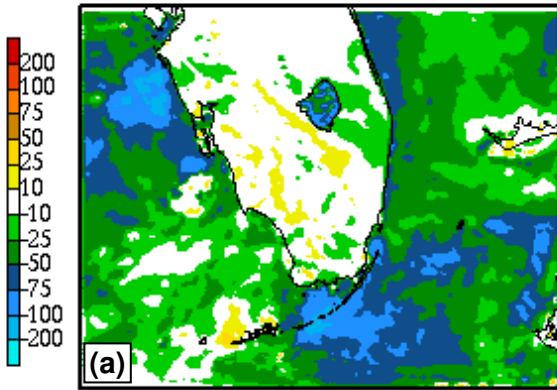**Figure 5.** Same as Figure 4 except for the bias scores.
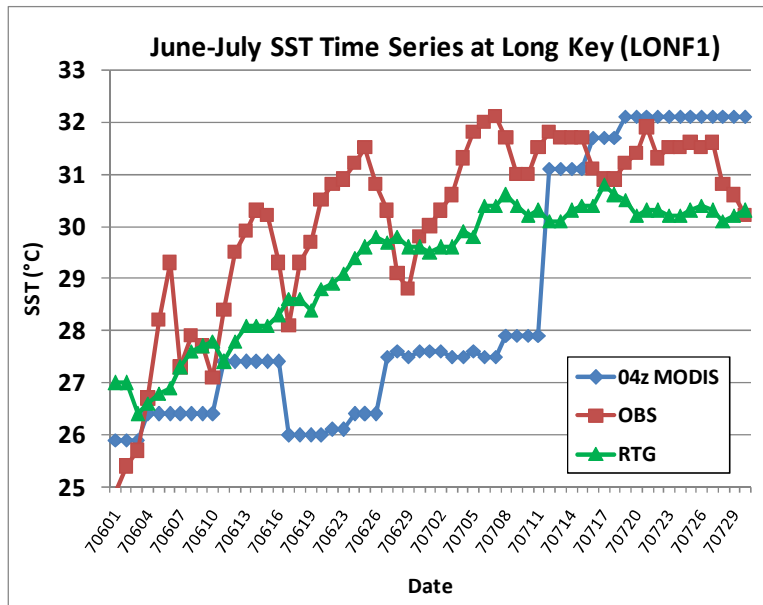
Figure 6. June–July 2007 time series of daily 0900 UTC observed SSTs at Long Key, FL (LONF1), daily RTG-initialized SSTs, and MODIS-initialized SSTs interpolated to station LONF1 from the 0400 UTC composite, according to the legend provided.
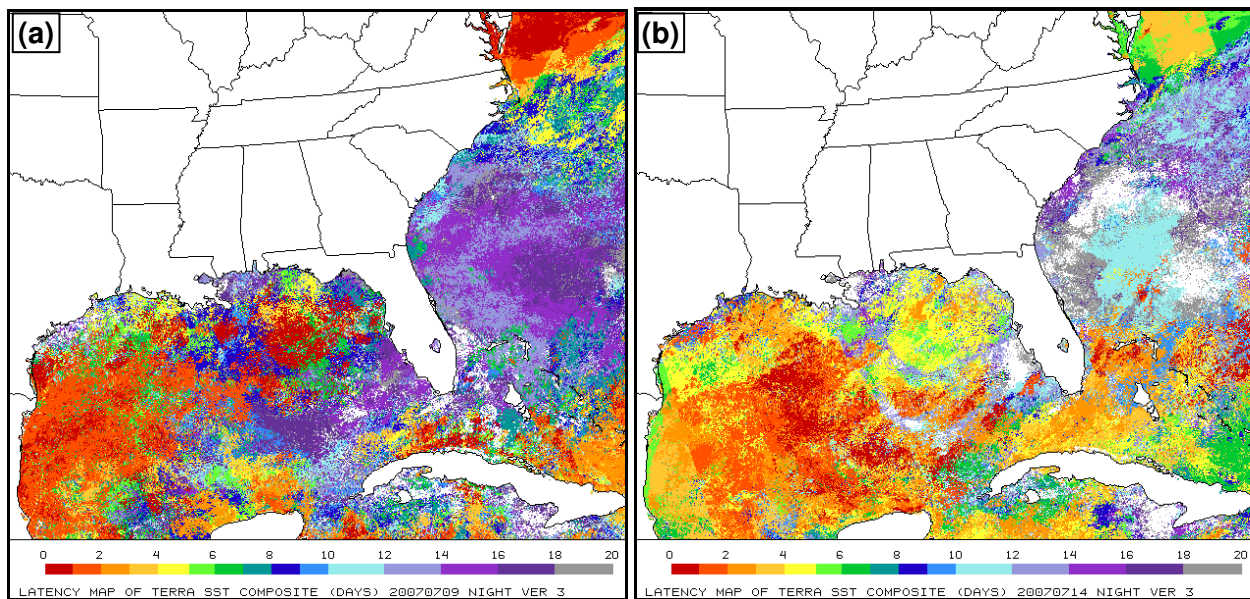
Figure 7. Latency of MODIS SST composite in days, according to the scale provided, valid for the 0400 UTC composite on (a) 9 July, and (b) 14 July. Notice the dramatically improved latency values around the Florida Keys by 14 July in (b).

Table 1. Summary of mean forecast SST (FBAR for MODIS and RTG), mean observed SST (OBAR), RMSE, bias, and corresponding MODIS composite for all 6 marine sites in each forecast cycle.

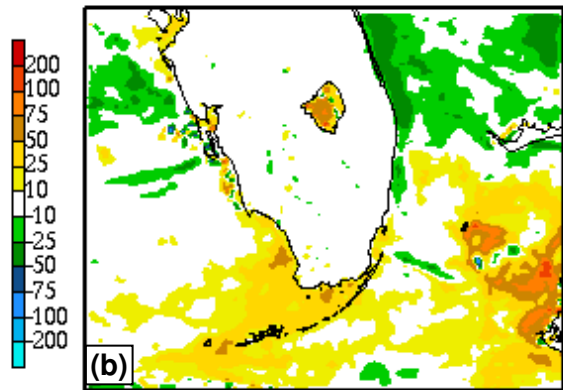| Forecast Cycle	*MODIS Composite*	FBAR MODIS	FBAR RTG	OBAR	RMSE MODIS	RMSE RTG	Bias MODIS	Bias RTG
0300 UTC	*1900 UTC*	26.9	27.0	26.8	1.1	1.2	0.1	0.1
0900 UTC	*0400 UTC*	25.8	26.7	26.3	1.3	1.3	-0.5	0.4
1500 UTC	*0700 UTC*	25.7	27.0	26.7	1.6	1.3	-0.9	0.3
2100 UTC	*1600 UTC*	26.4	26.7	26.9	1.2	1.4	-0.6	-0.2

Figure 8. WRF simulated latent heat flux differences (MODIS – RTG) valid at 0900 UTC 15 June for the (a) 18-h forecast initialized at 1500 UTC 14 June, and (b) 12-h forecast initialized at 2100 UTC 14 June.